Three-dimensional multi-level heat transfer model of silica aerogel

He LIU, Zeng Y. LI*, Xin P. ZHAO and Wen Q. TAO

* Corresponding author: Tel.: ++ (86)029-82665446; Fax: ++ (86) 029-82665445; Email: lizengy@mail.xjtu.edu.cn

Key Laboratory of Thermo-Fluid and Science and Engineering, Ministry of Education
School of Energy and Power Engineering, Xi'an Jiaotong University, Xi'an 710049, P.R. China

Abstract In this paper, a 3-D multi-level heat transfer model is developed in consideration of the tortuous path of heat conduction in solid skeleton and the fractal characteristic of silica aerogel. The heat conduction is analyzed for both the secondary particle model and the cluster model. The expression of effective thermal conductivity of a multi-level model is derived. The theoretical predictions from the proposed multi-level model are compared with three sets of experimental data with different densities and porosities. The results from the proposed model show good agreement with the experimental data.

Keywords: silica aerogel, DLCA, unit cell analysis, fractal model, effective thermal conductivity

1. Introduction

Silica aerogel has extraordinary properties resulting from its highly porous nanostructure such as low density, high porosity, large specific surface area and ultralow thermal conductivity. In particular, the low thermal conductivity characteristic of such aerogel has led to great interest in this material as a lightweight thermal insulator. Its microstructure can be partially controlled in producing process, which makes the study of relation between structural parameters and its effective thermal conductivity significant (Zeng et al., 1995).

Silica aerogel is known to exhibit a low density nanoscale pearl-necklace structure that consists of tangled strands of roughly spherical particles as shown in Fig.1 (Moner-Girona et al., 2003). These particles may themselves exhibit complex internal structure, and are usually considered to contain smaller spheres of bulk amorphous silica.

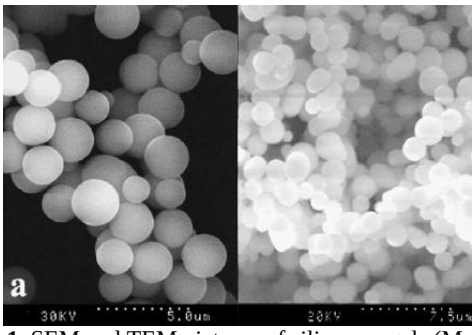

Fig. 1. SEM and TEM pictures of silica aerogels (Moner-Girona et al., 2003).

It is usually assumed that the medium has a periodic structure, and a unit cell or representative cell is often chosen for such a study. Based on this idea, different unit cell models to determine the effective thermal conductivity of such nanoporous media with periodic structures were developed (e.g. Zeng et al., 1995; Wei et al., 2011). Most recently, a great deal of attention has been given to the disordered nature of the micropores inside the secondary particles and the tortuous path of heat conduction in solid skeleton. A 3-D random nanoparticle aggregate structure was improved (Zhao et al., 2012) However, few note the influence of the tortuous path of heat conduction in solid skeleton. The tortuosity of the heat transfer path suggests that the fractal

theory may be used to predict properties of the nanoporous medium (e.g. Katz et al.,1985; Yu et al., 2002). In a recent paper, fractal model for the effective thermal conductivity of bidispersed porous media is developed and has shown good agreement with experimental data (Yu et al., 2002).

In this paper, in order to provide a microscopic understanding of the thermal behavior of silica aerogel, and to provide a predictive tool in the further development, we have constructed a multi-level model for amorphous silica aerogel. Diffusion-Limited Cluster Aggregation (DLCA) method is adopted to simulate the random secondary-nanoparticle aggregation structure and provide main structural parameters for the multi-level model. Furthermore, the predicted values are compared with three sets of experimental data and validated by further prediction of the effective thermal conductivity of silica aerogel.

2. Microstructure and fractal description of silica aerogel

The measure of a fractal object, $M(L)$, is governed by the scale L through a scaling law in the form of (Mandelbrot et al., 1982)

$$M(L) \sim L^{D_f} \tag{1}$$

The geometry structures such as Sierpinski gasket, Sierpinski carpet, and Koch curve are the examples of the exact self-similar fractals, which exhibit the self-similarity over an infinite range of length scales. However, the exactly self-similar fractals in a global sense are rare in nature. Although many objects found in nature (such as the coast lines of islands) are not exactly self-similar, they are statistically self-similar. These objects exhibit the self-similarity in some average sense and over a certain local range of length scales L.

Silica aerogel typically exhibits a complex structure; the smallest feature is a 'primary' particle of amorphous silica, typically 1-5nm in diameter. The primary particles aggregate to form 'secondary' particles, typically an order of magnitude larger, and these, in turn, form pearl-necklace structures whose details depend on the density (Fig.2, Good, 2006). There are two types of pores: pores between primary particles inside a secondary particle and pores between secondary particles inside a cluster. Both types of pores form irregular and tortuous pore channels. A cluster with various pore sizes can be considered as a bundle of tortuous capillary tubes with variable cross sectional areas, with diameter and tortuous length (actual length) being d_p and $L(d_p)$, respectively.

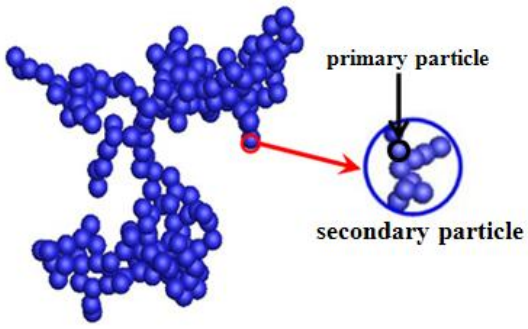

Fig. 2. Nanoparticle aggregation structure of silica aerogel.

Above all, the aerogel appears to exhibit fractal dimensionality, at least over a small length scales. The fractal dimension D_f used in this paper is referred to both the statistical and the exact fractals (Feder, 1988).

The total number N of channel pathways should follow the following scaling law

$$N\left(L \geq d_{p\min}\right) = \left(\frac{d_{p\max}}{d_p}\right)^{D_f} \tag{2}$$

where, d_p, $d_{p\ \min}$ and $d_{p\ \max}$ are the pore size, minimum and maximum size of pore. D_f is the area fractal dimension of a cross section normal to the heat flow direction.

Differentiating Eq. (2) results in the number of pores whose sizes are within the infinitesimal range between d_p and (d_p + d d_p),

$$-\mathrm{d}N = D_f d_{p\max}^{D_f} d_p^{-(D_f+1)} \mathrm{d}d_p \tag{3}$$

The negative sign in Eq. (3) implies that the pore (or chain) number decreases with the increase of pore (or chain) size.

The relation among the fractal dimension, porosity and scale for self-similarity in porous media has been derived analytically referring to the study of Yu and Li, 2001. The relation is given by

$$D_f = d - \frac{\ln \varphi}{\ln \frac{d_{p\min}}{d_{p\max}}} \tag{4}$$

where, d is the Euclidean dimension, d=2 and 3 in the two- and three- dimension spaces respectively. φ is the porosity of the porous media.

A simple geometry model for tortuosity of flow path in porous media also has been proposed referring to the study of Yu and Li, 2004. The model is expressed as a function of porosity and there is no empirical constant in the model. The real tortuosity can be obtained by average over all possible configurations for flow path in porous media. The averaged tortuosity is thus given by

$$\tau_{av} = \frac{1}{2}\left[1 + \frac{1}{2}\sqrt{1-\varphi} + \sqrt{1-\varphi} \times \sqrt{\left(1/\sqrt{1-\varphi} - 1\right)^2 + \frac{1}{4}} \Big/ \left(1 - \sqrt{1-\varphi}\right)\right] \tag{5}$$

And the tortuosity fractal dimension is expressed as

$$\frac{L_0}{d_{p\min}} = \frac{d_{p\max}}{d_{p\min}} \sqrt{\frac{\pi}{4} \frac{D_f}{2 - D_f} \frac{1-\varphi}{\varphi}} \tag{6}$$

$$D_T = 1 + \frac{\ln\left\{\left[\tau_{av}\left(D_f + D_T - 1\right)\right] / D_f\right\}}{\ln\left(L_0 / d_{p\min}\right)} \tag{7}$$

where, L_0 is the representative length.

3. DLCA simulation of structure of silica aerogel

Silica aerogel structure is obtained via sol-gel technique and the supercritical drying. DLCA occurs when there are negligible repulsive forces between the colloid particles, causing particles to stick upon contact and form highly tenuous structures (Good, 2006). We make use of off-lattice DLCA to simulate the random secondary-nanoparticle aggregation in the aerogel formation process.

At beginning, a certain number of particles determined by the porosity are inserted at random off-lattice points in the simulation region. Then, a picked particle or cluster moves with a small distance in a random direction. Whether the collision with other particles or clusters occurs depends on the movement. If it happens, the collision will cause the aggregation of a bigger cluster particles or clusters. If not, another particle or cluster will be chosen and moves. The process will repeat until all the particles merge into one cluster (Jullien et al., 1997).

4. 3D multi-level model for effective thermal conductivity of silica aerogel

Silica aerogel can be treated isotropically from macro perspectives although the micro structure is disorder. Generally, there only exists large temperature difference in one direction in actual working atmosphere. Thus, one-dimensional heat transfer model is often used to obtain the effective thermal conductivity of a certain material in most theoretical or experimental studies. In order to predict its thermal insulation performance, we have constructed a multi-level model for amorphous silica aerogel.

4.1 Effective thermal conductivity of the secondary particle

Since the sizes of primary particles are much smaller than that of the secondary particles or clusters, the effective thermal conductivity is an average quantity and not all aspects of the random microstructure need be induced to obtain the average thermal conductivity. For the purpose of the preliminary work, on the basis of the unit cell analysis, for simplicity, a secondary particle is considered as a periodical array of the unit cell which represents the main characteristics of the real structure of the primary particle. Here, we propose intersecting square rods as the unit cell model as shown in Fig.3 referring to the study of Zeng, Hunt and Grief, 1995.

We further suppose heat conduction is one dimensional in this model for the model is symmetric in the plane perpendicular to heat transfer direction.

$$\varphi_c = \left[a_0^3 + 3a_0^2\left(d_{p0} - a_0\right)\right] / d_{p0}^3 = 3\gamma_{a1}'^2 - 2\gamma_{a1}'^3 \tag{8}$$

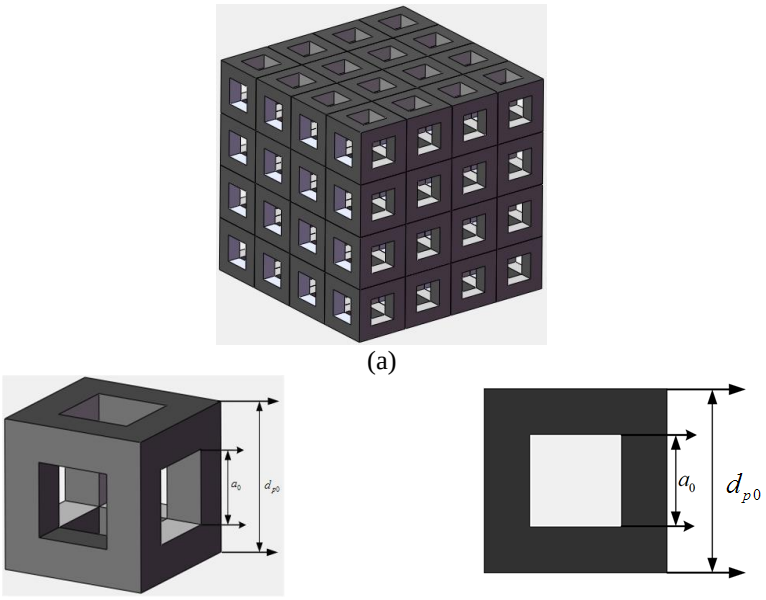

Fig. 3. The simplified model of a secondary particle (a) the packing structural pattern of unit cell models,(b) unit cell model of intersecting square rods,(c) the cross-section view for the unit cell model.

$$\gamma_{a1}^{'} = a_0 / d_{p0} \tag{9}$$

where, φ_c is the porosity of the secondary particle, $\gamma_{a1}^{'}$ represents the geometric length scale ratio, a_0 represents the pore size inside a unit cell model and d_{p0} is the length of the unit cell model.

The effective thermal conductivity of the secondary particle $k_{e,c}$ is then equal to

$$k_{e,c} = \sum Q / \left(\Delta T d_{p0} \right) \tag{10}$$

$$Q_1 = k_g \Delta T a_0^2 / d_{p0} \tag{11}$$

$$Q_2 = 4 k_s \Delta T \left[\left(d_{p0} - a_0 \right) / 2 \right]^2 / d_{p0} \tag{12}$$

$$Q_3 = 2 \Delta T a_0 \left(d_{p0} - a_0 \right) / \left[\left(d_{p0} - a_0 \right) / k_s + a_0 / k_g \right] \tag{13}$$

where, Q_1 represents heat transferred through the vertical rods; Q_2 represents heat transferred from the horizontal rods at the bottom through the gas to the horizontal rods at the top; Q_3 represents heat transferred by the gas inside the unit cell. k_g is the gaseous thermal conductivity in aerogels, k_s is the solid thermal conductivity in the nano-rods. Since k_s is not easy to measure, we often replace k_s with the bulk thermal conductivity k_{bulk}, 1.34W/m K, to simplify the calculation. The small pore sizes greatly restrict the motion of gas molecules and hence reduce the gaseous conduction. The gaseous thermal conductivity within nano-pore is given by Eq.(14) (Zeng et al., 1995).

$$k_g = \frac{60.22 \times 10^5 \, p T^{-0.5} \varphi_c}{0.25 S \rho_a \varphi_c^{-1} + 4.01 \times 10^9 \, p T^{-1}} \tag{14}$$

where, p is the ambient pressure (bar), T is the ambient temperature, ρ_a is the aerogel density and S is the specific surface area. The specific surface area is expressed as

$$S = \frac{6 \left(d_{p0}^{\,2} - a_0^2 \right)}{\rho_a d_{p0}^{\,2}} \tag{15}$$

4.2 Effective thermal conductivity of silica aerogel

We ignore the small-scale structure of the secondary particles and assume that the aerogel is formed by the larger-scale particles (secondary particles) by particle agglomeration. Then the effective thermal conductivity of the secondary particle, $k_{e,c}$ takes place of the solid thermal conductivity of the secondary particles or clusters.

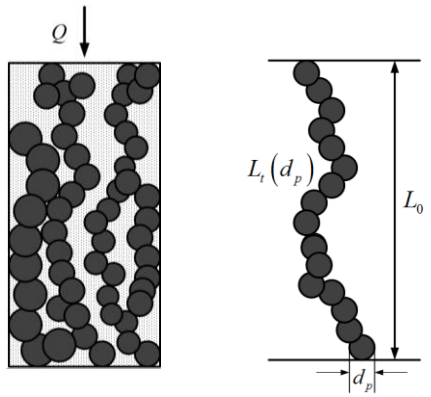

Fig. 4. Side view of structure of secondary particle aggregation and typical chain of secondary particles.

It can be seen from Fig.4 that in the structure of silica aerogel, some secondary particles contact each other to form chains whereas others do not concluded in any chain. These two configurations of secondary particles in the medium should be included in the model. Fig.4 shows the schematic of a chain of secondary particles with a total length of $L(d_p)$ that is greater than L_0, the representative length.

We refer to a mixed chain consisting of secondary particles and the gas enclosing these particles. In reality, the cross section of the chain may not be circular in shape, and the area and shape of cross section of each mixed chain may be different. We assume that the area distribution of cross section of mixed chains follows the same fractal power law as in Eq. (3).

We also assume in this model heat conduction is one-dimensional and that the heat flow lines approximately follow the chains. The effective thermal conductivity of the mixed chains and nontouching particles can be expressed as

$$k_e = \frac{A_n}{A} k_{e,n} + \left(1 - \frac{A_n}{A}\right) k_{e,mc} \qquad (16)$$

where, A is the total area of a representative cross section, and A_n is an equivalent area of a cross section which has the same porosity as the nontouching secondary particles.

For the effective thermal conductivity of three dimensional nontouching secondary particles, the expression is obtained referring to the study of Hsu, Cheng and Wong, 1995 as

$$k_{e,n} = k_g \left[1-(1-\varphi)^{2/3}\right] + \frac{k_g (1-\varphi)^{2/3}}{1+(1/\beta-1)(1-\varphi)^{1/3}} \quad , \beta = k_{e,c}/k_g \qquad (17)$$

The model in Fig.4 is adopted for the mixed chain in the direction perpendicular to the heat flow which only takes contact resistance between two adjacent secondary particles into consideration.

The thermal resistance of a unit cell of a secondary particle (shown in Fig. 5) which formed the chain is expressed as

$$R_{c1} = \frac{1}{\lambda}\left[\frac{\gamma_a}{2k_g\left(1-\gamma_a^{'}\right)+k_{e,c}\gamma_a^{'}} + \frac{\left(1-\gamma_a\right)\gamma_a^{'}}{k_g\left(1-\gamma_a^{'2}\gamma_c^2/\gamma_a^2\right)+k_{e,c}\gamma_a^{'2}\gamma_c^2/\gamma_a^2}\right] \qquad (18)$$

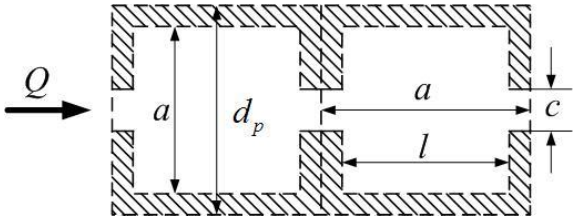

Fig. 5. Secondary particle- secondary particle system.

where, $\gamma_a = l/a$, $\gamma_a^{'} = a/d_p$ and $\gamma_c = c/l$ the geometric length scale ratio and contact length scale ratio at the microscale within a chain, respectively.

$$\varphi = 1-\left[\left(1-3\gamma_c^2\right)\gamma_a^3 + 3\gamma_c^2\gamma_a^2\right]\left(1-\varphi_c\right) \qquad (19)$$

where, φ is the porosity of the secondary-particle aggregate structure generated by DLCA.

To obtain the value of $\gamma_a^{'}$ in Eqs. (18) and (19), we refer to Fig. 6. Note that the porosity within a cluster is given by

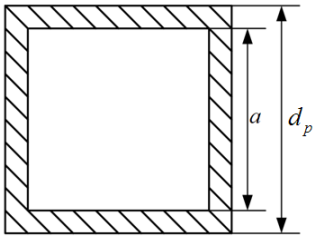

Fig. 6. A simplified cross section of a mixed chain of secondary particle.

$$\varphi = \left(d_p^2 - a^2 + a^2\varphi_c\right)/d_p^2 \quad (20)$$

$$\gamma_a^{'} = a/d_p = \sqrt{(1-\varphi)/(1-\varphi_c)} \quad (21)$$

For a mixed chain of a length $L_t(d_p)$, the thermal resistance can be obtained as

$$R_c = \frac{L_t(d_p)}{a} R_{c1} \quad (22)$$

Eq. (3) shows that in the interval d_p and d_p + dd_p, there are the parallel chains of (−dN). Then the total resistance of the mixed chains in the computational domain is expressed a

$$\frac{1}{R_{mc}} = -\int \frac{\mathrm{d}N}{R_c} \quad (23)$$

We obtain the effective thermal conductivity of the parallel chains in the computational domain by inserting Eq. (2), (3) and (20) into Eq. (23):

$$\begin{aligned} k_{e,mc} &= \frac{L_0}{A}\cdot\frac{1}{R_{mc}} \\ &= \frac{d_{p\max}^2}{A}\left(\frac{d_{p\max}}{L_0}\right)^{D_T-1}\frac{D_f}{1+D_T-D_f} \\ &\times\left\{1\Big/\left[\frac{\gamma_a/\gamma_a^{'}}{2k_g\left(1-\gamma_a^{'}\right)+k_{e,c}\gamma_a^{'}}\right.\right. \\ &\left.\left.+\frac{(1-\gamma_a)}{k_g\left(1-\gamma_a^{'2}\gamma_c^2/\gamma_a^2\right)+k_{e,c}\gamma_a^{'2}\gamma_c^2/\gamma_a^2}\right]\right\} \end{aligned} \quad (24)$$

where, $d_{p\max}^2/A$ is the ratio of the maximum area of cross section of a mixed chain to the representative area A, and $d_{p\max}/L_0$ is the ratio of the maximum diameter of cross section of a mixed chain to the representative length L_0 along the heat flow direction.

Because the microstructure of silica aerogel is very complex, the ratios $d_{p\max}/d_{p\min}$, A_n/A, $d_{p\max}^2/A$, $d_{p\max}/L_0$ and γ_c cannot be determined analytically, we give these values by empirical estimation and statistical results of structure generated by DLCA.

5. Results and discussion

The measured porosity of silica aerogel is usually obtained by

$$\varphi_a = 1-\rho_a/\rho_s \quad (25)$$

The relation among the porosity of the secondary particle, the porosity of the secondary-particle aggregation and the measured porosity of silica aerogel is expressed as

$$\varphi_c = \left(\varphi_a - \varphi\right)/\left(1-\varphi\right) \quad (26)$$

In order to prove the feasibility of the multi-level heat transfer model, the comparison between the present results and three sets of experimental data from Zeng et al.(1995), Zhang et al.(2013) and Wei et al. (2011) are shown in Fig.8, Fig.9 and Fig.10. For comparing the effective thermal conductivity obtained by the multi-level model with available experimental data, we generated three sets of structures by DLCA as shown in Fig.7. The structural parameters are listed in Table 1.

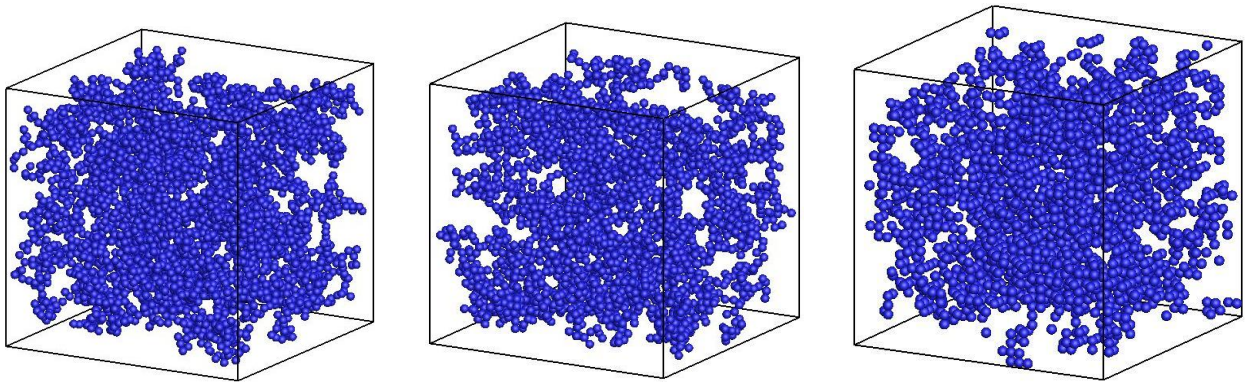

(a) (b) (c)

Fig. 7. Secondary particle distribution in the computational domain for different density and porosity. (*a*) φ=89%, ρ_a = 110 kg/m^3; (*b*) φ=83.5%, ρ_a = 240 kg/m^3 (*c*) φ=95%, ρ_a = 114 kg/m^3.

Table1 Structural parameters for model1, model2 and model3.

model	Porosity	porosity of DLCA structure	density (kg/m^3)	d_{pmax}/d_{pmin}	A_n/A	d_{pmax}^2/A	d_{pmax}/L_0	γ_c
model1 for Zeng	0.94	0.890	110	1/0.100	0.2	0.055	0.10	0.30
model2 for Zhang	0.89	0.835	240	1/0.070	0.3	0.095	0.20	0.40
model3 for Wei	0.95	0.900	114	1/0.085	0.2	0.066	0.10	0.37

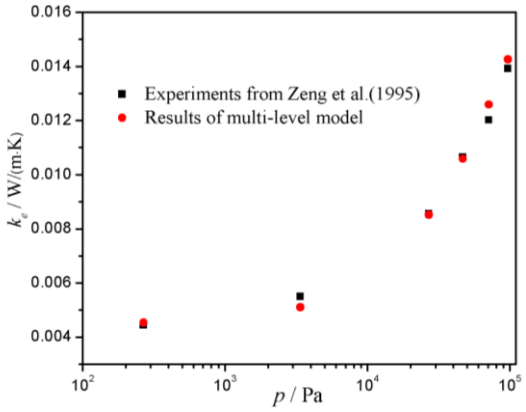

Fig. 8. Comparison between the effective thermal conductivities of the multi-level model and Zeng's experimental data.

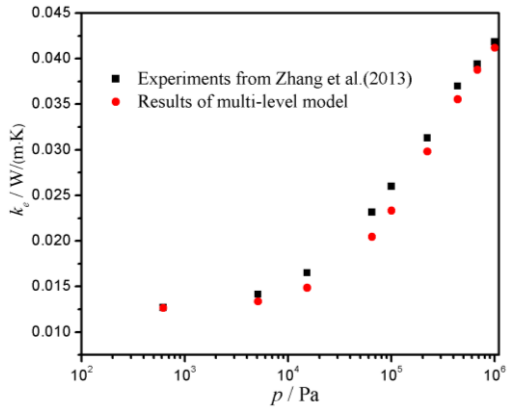

Fig. 9. Comparison between the effective thermal conductivities of the multi-level model and Zhang's experimental data.

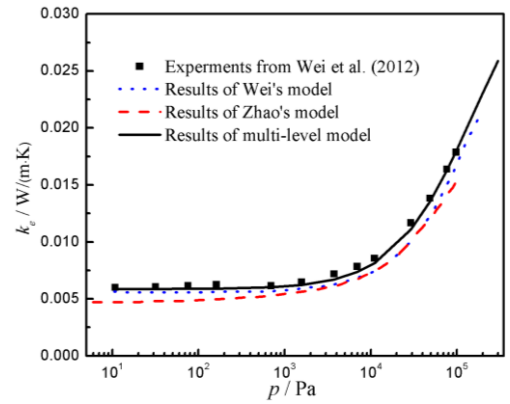

Fig. 10. Comparison among the effective thermal conductivities of the multi-level model, Wei's model and Zhao's model.

Figs.8, 9 and 10 show the comparisons between the experimental data and the results of the multi-level model under different pressures at ambient temperature. The three figures show the same change trend. The value of the thermal conductivity contains three parts: solid thermal conductivity, gaseous thermal conductivity and radiation thermal conductivity. The radiation can be ignored at ambient temperature and the solid thermal conductivity keeps constant although the pressure changes. When the pressure is low ($<10^4$ pa), the heat transfer from gas can be ignored because the motions of gas molecules are constrained remarkably. As the pressure increases, the mean free path of gas molecules decrease and the restrictions of solid skeleton are reduced. Thus, we can see that the total thermal conductivity increases with the increasing pressure. The comparisons indicate that the validity of the present model for that it gives almost the same satisfactory results with the deviation within 19.8% in the tested pressure range.

The precision of a model can be reflected from the predicted results at low pressure. For earlier existing heat transfer models, main concerns are given to the heat transfer mechanism of solid skeleton and the couple effect between gas and solid particles. Fig.10 also shows the comparison among results from the present model, results referring to the model of Zhao et al. (2012) and Wei et al. (2011). Because more details are considered, it is found that the present model agrees better than other theoretical models for the entire tested pressure range, especially at low pressure.

Finally, the 3D multi-level model is proved to be more realistic for the random or disordered nanoporous media. This is because nanoporous media such as silica aerogel

consisting of uniform particles or regular structure are rarely found in nature. This paper presents a systematic analysis of the effective thermal conductivity of silica aerogel. However, the present model is more complex compared with the conventional method of unit cell analysis for the estimation of the parameters such as A_n/A, $d_{p\max}^2/A$ and $d_{p\max}/L_0$ is not easy.

6. Conclusion

This paper has derived a 3D multi-level model based on the fractal characteristics of the microstructures of silica aerogel and on the electrical analogy technique. The proposed 3D multi-level model is a function of the tortuosity fractal dimension, area fractal dimension, porosity, ratios of areas, length scale, and contact length. The 3D multi-level model is compared with three sets of experimental data and other models. The results show good agreements. The 3D multi-level model may be particularly useful for the random nanoporous media with nonuniform particles or clusters.

Note that we have assumed one-dimensional heat conduction in the unit cell, and the heat flow lines approximately follow the chains for simplicity purposes in this paper. In reality, the lateral heat conduction, that is, two-dimensional heat conduction should be considered for a better modeling. And the size effect of the solid thermal conductivity is neglected in the present work. These aspects will be considered in our future work.

Acknowledgements

The present work is supported financially by National Natural Science Foundation of China under Grant Nos. 51276138.

Reference

Zeng, S.Q., Hunt, A., Grief, R., 1995. Geometric Structure and Thermal Conductivity of Porous Medium Silica Aerogel. J. Heat Transfer 117(4), 1055–1058.

Moner-Girona, M., Roig, A., Molins, E., Llibre, J., 2003. Sol-Gel Route to Direct Formation of Silica Aerogel Microparticles Using Supercritical Solvents. J. Sol-Gel Sci. Technol. 26(1–3), 645–649.

Wei, G.S., Liu, Y.S., Zhang, X.X., Yu, F., Du, X.Z., 2011. Thermal conductivities study on silica aerogel and its composite insulation materials. Int. J. Heat Mass Transfer 54 (11–12), 2355–2366.

Zhao, J.J., Duan, Y.Y., Wang, X.D., Wang, B.X., 2012. A 3-D numerical heat transfer model for silica aerogels based on the porous secondary nanoparticle aggregate structure. J. Non-Cryst. Solids 358(10), 1287–1297.

Katz, A.J., Thompson, A.H., 1985. Fractal sandstone pores: implications for conductivity and pore formation. Phys. Rev. Lett. 54, 1325–1328.

Yu, B., Cheng, P., 2002. A fractal permeability model for bi-dispersed porous media. Int. J. Heat Mass Transfer 45, 2983–2993.

Yu, B.M., Cheng, P., 2002. Fractal models for the effective thermal conductivity of bidispersed porous media. J. Thermophys Heat Transfer 16(1), 22–29.

Mandelbrot, B.B., 1982. In: The fractal geometry of nature. W.H. Freeman, New York, 23–57.

Good, B.S., 2006. Structure and thermal conductivity of silica aerogels from computer simulations. In: A.O.C.F.C.O.J. Dillion (Ed.) Hydrogen Cycle-Generation, Storage and, Fuel Cells, 227–232.

Feder, J., 1988. In: Fractals. Plenum, New York, 8–14.

Yu, B.M., Li, J.H., 2001. Some fractal characters of porous media. Fractals 9(3), 365–372.

Yu, B.M. and Li, J.H., 2004. A geometry model for tortuosity of flow path in porous media. Chin. Phys. Lett. 21, 1569–1571

Jullien, R., Hasmy, A., Anglaret, E., 1997. Effect of cluster deformations in the DLCA modeling of the sol-gel process. J. Sol-Gel Sci. Technol. 8(1–3), 819–824.

Zeng, S.Q., Hunt, A., Grief, R., 1995. Transport properties of gas in silica aerogel. J. Non-Cryst. Solids. 186, 264–270.

Hsu, C.T., Cheng, P., Wong, K.W., 1995. A lumped-parameter model for stagnant thermal conductivity of spatially periodic porous media. J. Heat Transfer 117(2), 264–269.

Zhang, H., Li, Z.Y., Dan, D., Tao, W.Q., 2013. Influence of pressure on the effective thermal conductivity of nanoporous materials. J. ENG THERMOPHYS-RUS 34(4), 756–759(In Chinese).